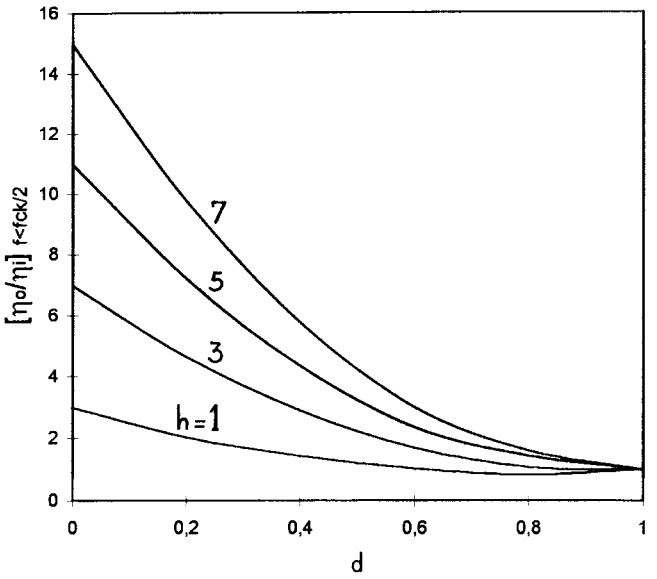

Fig. 7. White-noise power spectral density transfer function of a simple T/H for f $< f_{\rm ck}/2$, where **d** is the track pulse duty cycle and **h** the closest integer to $B_{\rm wn}/f_{\rm ck}$, and where the worst case occurring at $f = 0$ was assumed.

filtering. The maximum offset cancellation achievable is limited by the T/H mismatchings and by the adder accuracy.

For avoiding excessive staircase ripple on the output waveform, the input signal spectrum bandwidth should be preferably smaller than 0.2 times the Nyquist frequency. Otherwise a postchopper LP filter may be required.

Finally, these demodulators show a white-noise degradation due to the hold function; this degradation being minimum for the maximum allowable duty cycle of 0.5 and minimum amplifier bandwidth.

ACKNOWLEDGMENT

The authors would like to thank D. Barrettino, of Electrónica Bilotti, for his helpful suggestions.

REFERENCES

[1] K. Hsieh *et al.*, A low-noise chopper stabilized differential switched-capacitor filtering technique, *IEEE J. Solid-State Circuits*, vol. SC-16, no. 6, pp. 708–715, Dec. 1981.

[2] C. C. Enz *et al.*, A CMOS chopper amplifier, *IEEE J. Solid-State Circuits*, vol. SC-22, pp. 335–341, June 1987.

[3] C. C. Enz and G. C. Temes, "Circuit techniques for reducing the effects of op-amp imperfections: Autozeroing, correlated double sampling, and chopper stabilization," *Proc. IEEE*, vol. 84, pp. 1584–1613, Nov. 1996.

[4] C. Menolfi and Q. Huang, A low-noise CMOS instrumentation amplifier for thermoelectric infrared detectors, *IEEE J. Solid-State Circuits*, vol. 32, pp. 968–976, July 1997.

[5] A. Bilotti *et al.*, Monolithic magnetic hall sensor using dynamic quadrature offset cancellation, *IEEE J. Solid-State Circuits*, vol. 32, pp. 829–836, June 1997.

[6] J. S. Fischer, Noise sources and calculation techniques for switched capacitor filters, *IEEE J. Solid-State Circuits*, vol. SC-17, pp. 742–752, Aug. 1982.

[7] C. Gobet, "Spectral distribution of a sampled first order lowpass filtered white noise," *Electron. Lett.*, vol. 17, no. 19, pp. 720–721, Sept. 1981.

[8] C. Gobet and A. Knob, "Noise analysis of switched capacitor networks," *IEEE Trans. Circuits Syst.*, vol. CAS-30, pp. 37–43, Jan. 1983.

Experimental Chua's Circuit Arrays As an Autowave Simulator

M. Gómez-Gesteira, M. deCastro, V. Pérez-Villar, and L. O. Chua

***Abstract*—A two-dimensional (2-D) array of electronic circuits is used to simulate the typical autowaves experimentally found in various active media (target and spiral waves). This experimental setup allows us to obtain some of the phenomena previously described in continuous media, but with a complete control on each cell and on the connections among them.**

***Index Terms*—Autowaves, electronic simulator, nonlinear circuits.**

I. INTRODUCTION

Autowaves are a type of waves characteristic of strongly nonlinear active media [1]. Typical examples include waves of combustion, phase transitions [2], waves of concentration in chemical reactions [3], and many different biological media (cardiac tissue [4], retina [5], and cultures of the slime mold *Dictiostelium Discoideum* [6]). Autowaves differ from classical waves in conservative media because they propagate at the expense of energy stored in the medium (for a complete description of autowave behavior and properties see Krinsky's seminal work [1]).

During the last decades, autowaves have become a common subject of research. In particular, the so-called target and spiral waves have been widely treated. A target wave, also called a pacemaker, is constituted by a series of circular waves spreading from a common origin with a certain wavelength and period. A spiral wave, also called vortex or reentry, is characterized by a self-sustained activity due to the rotation of a free end (tip) around a zone called the core. This core can be a piece of unexcitable medium or just a functional defect, i.e., a region where the tip cannot penetrate due to the refractoriness generated by the previous wave. Both kinds of waves are usually associated with waves observed in biological systems, mainly in cardiac muscle. The periodic firing of some specific cells in the sine-atrial node, which fixes the heart rhythm, can be compared with a target, and spiral waves are believed to be the origin of life-threatening arrhythmias in cardiac tissue [7]–[9].

For years, many continuous systems (e.g., Belousov-Zhabotinsky (BZ) reaction [3], catalitic surfaces [10], and *Dictiostelium Discoideum* populations [11]) have been the paradigm for studying autowave behavior.

Recently, some authors have stressed the important fact that some of the behaviors observed in cardiac tissue depend on its discrete nature [12], [13], which cannot be described by a continuous media (for a complete description of discrete media properties see [14]). This observation suggests the need to find an alternative autowave simulator to complement the information provided by direct research carried out by cardiologists.

Manuscript received November 17, 1997; revised August 19, 1998. This work was supported in party by the Commission Interministerial de Ciencia y Tecnologia under Project DGCICYT-PB94-0623 and the Conselleria de Educacion e Ordenacion Universitaria, Xunta de Galicia under Project XUGA-20602B97. This paper was recommended by Associate Editor B. E. Shi.

M. Gómez-Gesteira, M. deCastro, and V. Pérez-Villar are with the Group of Nonlinear Physics, Faculty of Physics, University of Santiago de Compostela, 15706 Santiago de Compostela, Spain.

L. O. Chua is with the Department of Electric Engineering and Computer Sciences, University of California, Berkeley, Berkeley, CA 94720 USA.

Publisher Item Identifier S 1057-7122(99)02757-9.

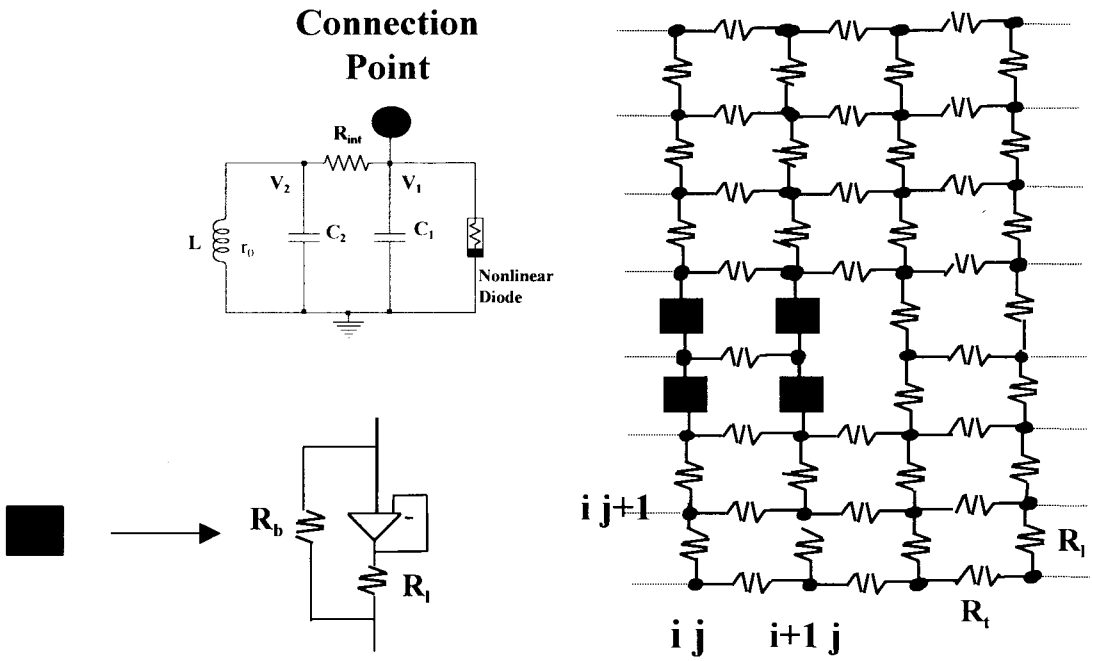

Fig. 1. Experimental setup. Dashed lines represent the rest of the array that is not represented for the sake of clarity.

During the last few years, some authors [15]–[17] have shown the possibility to obtain numerically target and spiral waves in an array of electronic circuits. Nevertheless, little had been done experimentally until recently, when some authors started considering a one-dimensional (1-D) array of circuits [18], [19] or a couple of parallel fibers [20], [21].

The aim of this paper is to reproduce most of the autowaves from continuous media in a discrete medium, a two-dimensional (2-D) array of electronic circuits. The experimental setup is described in Section II and different autowaves are shown in Section III. In Section IV, Chua's circuits are compared to the classical BZ reaction for autowave study.

II. Experimental Setup

In this section we will first describe the setup necessary to generate a spiral wave, since the setup necessary to obtain other autowaves can be obtained by simplifying this one. A sketch of a 2-D array (10×8 circuits) is shown in Fig. 1. Every cell in the array (a dark spot in Fig. 1) is a Chua's circuit [22], [23], whose parameters are summarized in Table I. With that set of parameters every circuit behaves as an excitable cell [16], [17], [21] which can be adjusted to a behavior $1:2$ at a frequency of 10.5 kHz following the method described in [19]. From now on, we will identify every circuit in the array by two indexes ij (i in X direction and j in Y direction). The origin, 11, will be considered at the lower left corner. Most of the circuits are coupled through resistances at node V_1. Two different resistances were considered, a longitudinal resistance $R_l = 4.7\ k\Omega$ which couples the Chua's circuits in the Y direction and a transversal resistance $R_t = 5.6\ k\Omega$ which couples the Chua's circuits in the X direction (we have considered $R_t > R_l$ to mimic an experimental fact observed in some biological media as cardiac tissue). The wave velocity in a certain direction was calculated dividing the number of circuits in that direction by the time the signal takes to propagate from first to last circuit ($V_l = 9.03 \times 10^4$ circuit/s in the Y direction and $V_t = 6.88 \times 10^4$ circuit/s in the X direction). Experimentally, a wave train with frequency 1 kHz was delivered by a pulse generator (Hewlett-Packard 33 120A) at the beginning of the array (at node V_1) and measured at the end of the array by an oscilloscope (Hewlett-Packard 54601, at a rate of 20 MSa/s) connected at node V_1. The square pulses (amplitude 6.0 V) delivered by the pulse generator at circuit 61 [Fig. 2(a)] trigger the medium and give rise to the sequence of waves shown in Fig. 2(b) for circuit 68. Note that at a frequency of 1 kHz, there is no interaction between consecutive waves: a wave is not modified by the refractory tail created by the previous one. It is a well-known fact that wave velocity decreases when decreasing the distance between two consecutive waves due to the dispersion relation [24], [25]. Actually, there is a critical period below which two consecutive pulses cannot generate two consecutive waves. That period, $T_r = 110\ \mu$s is called the refractory period.

TABLE I
Chua's Circuit Parameters

Parameter	Value	Tolerance
C_1	1 nF	5 %
C_2	100 nF	5 %
L	10 mH	10 %
R_{int}	270 Ω	1 %
r_0	10 Ω	
R_l	4.7kΩ	1 %
R_t	5.6kΩ	1 %
R_b	100kΩ	1 %

The first step to generate a spiral wave is to create an obstacle in the medium. This is experimentally achieved by uncoupling some of the circuits in the array both longitudinally and transversally. Nevertheless, to generate a spiral wave it is necessary to create a free end. A simple obstacle only splits the initially continuous wavefront into two waves rotating around the obstacle in opposite directions. These two waves collide and annihilate each other, giving rise to a continuous wave front after leaving the obstacle. To

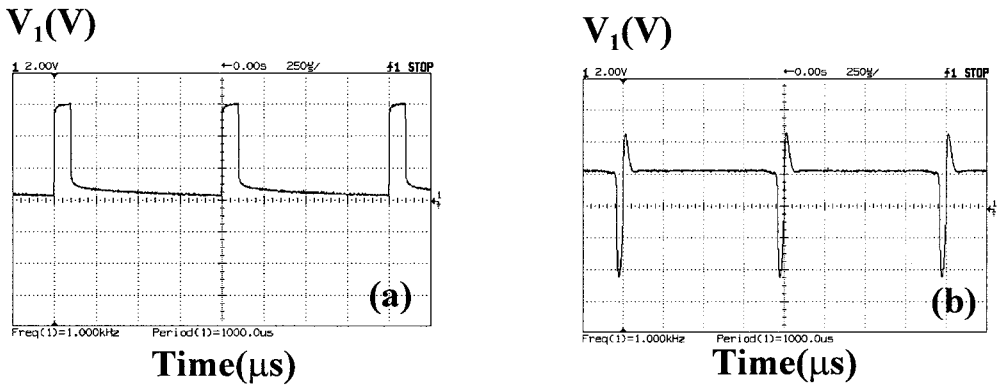

Fig. 2. (a) Wave train delivered by the pulse generator with an amplitude of 6.0 V and a frequency of 1.0 kHz. (b) Wave train measured at circuit 68 (the pulse generator had been connected at circuit 61).

generate a discontinuous wavefront (a free end) it is necessary to induce directional propagation. This property, experimentally found in cardiac tissue [26], [27], induces a different propagation in the OY^+ and in the OY^- direction. This is experimentally achieved by the element represented by a black square in Fig. 1. It consists of an operational amplifier circuit (TL084) and a resistance R_l in parallel with a resistance R_b ($R_b \gg R_l$ and R_t). For upward propagation the operational amplifier circuit stops the signal, which can only pass through R_b. For downward propagation the signal can use both channels (the operational amplifier circuit and R_b) in such a way that the equivalent resistance is $R_e \approx R_l$ since $R_b \gg R_l$. Note that, despite the fact that the voltage between consecutive circuits does not depend on the resistance between them, the intensity circulation through the equivalent resistance can stop propagation. Thus, when the wave arrives at the circuit ij the signal remains above the excitation threshold for a short time (around 30 μs). If the equivalent resistance between circuits ij and $ij+1$ is big (Rb), the intensity circulating through the element cannot charge the capacitor C_1 during the short period above mentioned. On the contrary, for downward propagation, the circuit ij can charge the capacitor C_1 in circuit $ij-1$ due to the small resistance (R_l).

Signal reconstruction in a 10×8 array is an arduous task since all circuits cannot be sampled simultaneously. To overcome this fact, the process to create a spatially extended image is as follows.

1) A certain circuit in the array is considered as the control point (channel one).
2) The rest of the channel (from two to four) can be used to measure simultaneously three circuits in the array.
3) The rest of the circuits in the array are measured in three's simultaneously.
4) Due to the periodicity of the events under scope, all signals can be scaled from a common point (e.g., taking the minimum of a wave in channel one as the initial time).
5) Then, fixing a time instant, the circuits a voltage above a certain threshold were plotted in dark color.

III. Experimental Results

To generate a target wave, the previously described setup was modified as follows. The circuits inside the obstacle were coupled by resistances R_l and R_t and operational amplifier circuits were removed in such a way that the medium became homogeneous. The pulse generator was connected at circuit 11. Waves started propagating from that corner to the rest of the medium, as shown in Fig. 3 where the minimum of the wave is plotted at three different times during propagation ($t_1 = 0$ μs, $t_2 = 80$ μs, and $t_3 = 120$ μs).

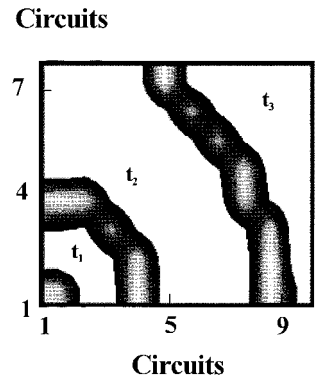

Fig. 3. Isochron lines corresponding to the minimum of a target wave measured at $t_1 = 0$ μs, $t_2 = 80$ μs, and $t_3 = 120$ μs after pulse deliverance at circuit 11.

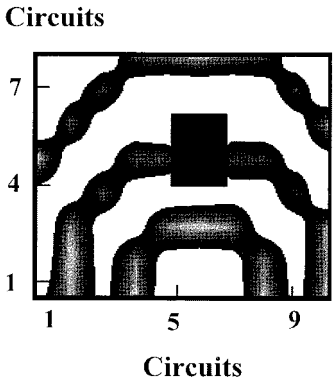

Fig. 4. Isochron lines corresponding to the minimum of a target wave measured at $t_1 = 36$ μs, $t_2 = 60$ μs, and $t_3 = 95$ μs after pulse deliverance at circuit 61. An obstacle was generated by uncoupling the circuits placed inside the rectangle $54 \rightarrow 56 \rightarrow 76 \rightarrow 74 \rightarrow 54$.

As mentioned in Section II, the existence of an obstacle is not enough to create a spiral wave. The circuits inside the rectangle $54 \rightarrow 56 \rightarrow 76 \rightarrow 74 \rightarrow 54$ were uncoupled from the rest. Once again, the minimum of the wave was plotted at three different times (Fig. 4). At $t_1 = 36$ μs, the wave generated by the pulse generator at location 61 has not yet arrived at the obstacle (shaded area). At $t_2 = 60$ μs the wave is crossing through the obstacle. The initially continuous wavefront has split into two waves rotating around the obstacle in opposite direction. At $t_3 = 95$ μs the wave has surpassed the obstacle and recovers its previous continuity.

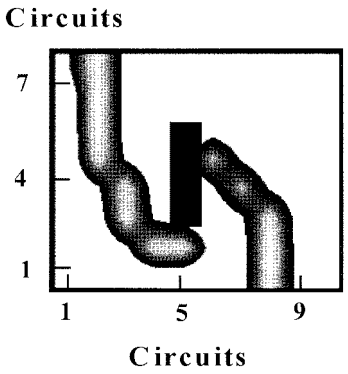

Fig. 5. Isochron lines corresponding to the minimum of a counter clockwise spiral wave measured at two different instants during a rotation period ($T = 186.5\ \mu$s). The spiral rotates steadily around the obstacle placed inside the rectangle $52 \rightarrow 56 \rightarrow 66 \rightarrow 62 \rightarrow 52$. The time delay between both rotation states is $75\ \mu$s.

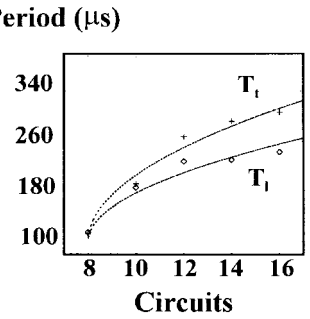

Fig. 6. Spiral period dependence on the extent of the obstacle. The size of the obstacle in one direction is considered to be constant but increases in the other direction. Crosses represent increasing size in the transversal direction and diamonds in the longitudinal direction. In both cases, the period increases with the extent of the obstacle.

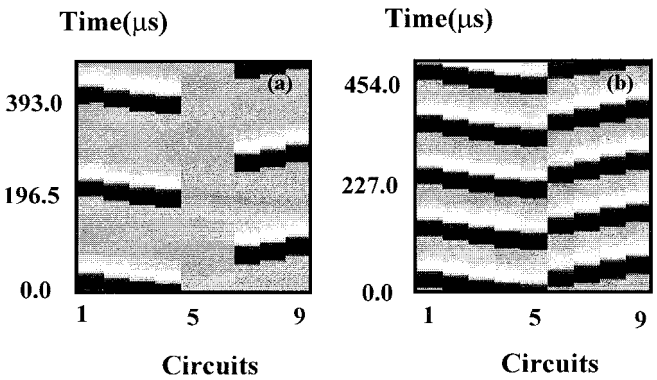

Fig. 7. Density plot X–T corresponding to a spiral wave. (a) Wave rotating around an obstacle. (b) Wave rotating around its own core.

Directional properties of the medium were imposed by means of the previously described element (black squares in Fig. 1). The pulse generator was placed at location 61 and an obstacle was created inside the rectangle $52 \rightarrow 56 \rightarrow 66 \rightarrow 62 \rightarrow 52$. The wave spreading from circuit 61 starts propagating northward. When it reaches the obstacle it can propagate on the right hand side but not on the left, due to propagation failure [13]. A part of the wave follows the obstacle boundary till the end of the obstacle where it can propagate in all directions. Therefore, one of the ends of the wave moves from location 56 to location 66, where it can propagate southward since the medium is homogeneous (except at the obstacle) for waves moving in the OY^- direction. The wave attains the lower left corner of the obstacle and can restart the cycle if the rotation period around the obstacle is longer than the refractory period of the medium. This gives rise to a self-sustained activity (reentry) around the obstacle. If the reentry frequency is shorter than the pulse-generator frequency, this external source is overwhelmed and can be switched off because it does not affect the reentry when placed far enough from the obstacle [21]. A spiral wave rotating with period $T = 186.5 \pm 0.5\ \mu$s around an obstacle is shown in Fig. 5, at two different times. The shaded area represents the obstacle.

The spiral period depends strongly on the obstacle size both in the X and in the Y directions. The difference between both directions depends on the anisotropy of the medium as shown in Fig. 6. In both cases, the extent of the obstacle in one direction was considered to be two circuits and increased in the other direction (crosses represent increasing size in the transversal direction and diamonds in the longitudinal direction). In both cases, the reentry period T increases nonlinearly with the obstacle perimeter l. In general, $T = l/V$ gives a linear dependence of T in l if V is assumed to be constant. Nevertheless, in our experiments l is small and V is itself a function of l due to the dispersion relation [24], [25].

As reported in cardiology [4], [7]–[9] and corroborated in other media [28], a spiral can rotate both around its own core and around an obstacle. Once the spiral had anchored at the obstacle and was rotating in a stationary way, the obstacle was filled with resistances and the operational amplifier circuits removed. After a brief transient, the spiral attained a new period and remained stationary. In an X–Y plot such as the one shown in Fig. 5, the new situation does not differ from the previous one since the spiral core behaves as a functional obstacle. The difference between both cases is best described by the space–time representation of Fig. 7. In this figure, the voltage was plotted as a function of time along a line crossing through the spiral core (the line $i4\ \forall i \in [1,\ 10]$). In Fig. 7(a) (spiral rotating around an obstacle), starting approximately in the middle of the space axis, dark strips of minimum voltage are observed spreading alternatively to the right and to the left. The delay between two consecutive dark strips on the same side is equal to 196.5±0.5 μs, which corresponds to the spiral period. Note that dark strips on the right side are not exactly placed between two consecutive strips on the left side, because the chosen line did not cross through the center of the core (the obstacle is placed inside the rectangle $43 \rightarrow 47 \rightarrow 77 \rightarrow 73 \rightarrow 43$). Central lines do not change their color in time since they lay inside the obstacle. The same situation is plotted in Fig. 7(b) for a spiral rotating around its own core. Note that in this case all points vary in time, but not simultaneously, due to the refractory properties of the medium after the passage of a wave. In this case the rotation period ($T = 113.5 \pm 0.5\ \mu$s) is considerably shortened when compared with spiral rotating around an obstacle. The spiral has accommodate its period to a value close to T_r previously defined. Note that, in this case, kinematical theory [24] predicts spiral movement under small external perturbations in a small medium [29]. Nevertheless, such a movement was not observed in our experiments, possibly due to the discrete nature of our medium which can give rise to spiral pinning even in absence of a physical obstacle (the spiral is anchored to the net).

IV. Conclusion

In the previous sections we have described how the typical autowaves observed in other media can be reproduced by means of a 2-D array of Chua's circuits. Some phenomena that can be observed in various experimental active media (e.g., anisotropy or existence of

TABLE II
COMPARISON BETWEEN A CONTINUOUS MEDIUM AND A 2-D ARRAY OF CHUA'S CIRCUITS

Phenomenon	Continuous Medium	Chua's Circuits
Anisotropy	+	+
Inhomogeneity	+	+
Directionality	-	+
Propagation Failure	-	+
Cell Control	-	+
Big Media	+	-
Moderate Cost	+	-

inhomogeneities) can also be obtained. Nevertheless, directionality, which is a property usually found around damaged regions in cardiac tissue [26], [27], can be reproduced in an array of electronic circuits but not in continuous media. In addition, the circuit medium allows us to control each cell and the connection among them in an independent way, which cannot be easily achieved in continuous media.

Unfortunately, an array of electronic circuits presents some disadvantages from a technical point of view. Whereas all points in a 2-D continuous medium (e.g., Belousov–Zhabotinsky (BZ) reaction [3], catalitic surfaces [10], and *Dictiostelium Discoideum* populations [11]) can be simultaneously recorded by a single snapshot, it is difficult to scan simultaneously a 10×8 array, whose elements have a time scale around 100–200 μs.

In summary, Table II establishes the similarities and differences between a continuous medium and an array of electronic circuits. It cannot be claimed that one of them is the most suitable for autowaves study, the better choice depends on the phenomenon being observed. Consequently, both media complement each other rather well as autowave simulators.

ACKNOWLEDGMENT

The authors wish to thank Dr. V. Perez-Muñuzuri, E. Sánchez, and S. Veiga-Solla for a careful reading of the manuscript and helpful suggestions. They also wish to thank C. Rico for his help with the experimental setup.

REFERENCES

[1] V. I. Krinsky, *Self Organization: Autowaves and Structures Far from Equilibrium,* V. I. Krinsky, Ed. Berlin, Germany: Springer–Verlag, 1984, pp. 9–19.
[2] Y. Kuramoto, *Chemical Oscillations, Waves and Turbulence.* Berlin, Germany: Springer–Verlag, 1984.
[3] A. N. Zaikin and A. M. Zhabotinsky, "Concentration wave propagation in two-dimensional liquid phase self-organizing system," *Nature,* vol. 225, pp. 535–537, 1970.
[4] M. A. Allesie, F. I. M. Bonke, and T. Y. G. Scopman, "Circus movement in rabbit atrial muscle as a mechanism in tachycardia," *Circ. Res.,* vol. 33, pp. 54–62, 1973.
[5] N. A. Gorelova and L. Bures, *J. Neurobiol.,* vol. 14, pp. 353–363, 1983.
[6] A. Robertson and A. F. Grutsch, *Cell,* vol. 24, pp. 603–611, 1983.
[7] G. R. Mines, "On circulating excitations in heart muscles and their possible relation to tachycardia and fibillation," *Trans. R. Soc. Can.,* vol. 4, Sec. 5, pp. 43–53, 1914.
[8] T. Lewis and A. M. Master, *Heart,* vol. 12, pp. 209, 1925.
[9] J. Jalife, Ed., "Mathematical approaches to cardiac arrhythmias," *Ann. N. Y. Acad. Sci.,* vol. 591, 1990.
[10] M. Bar, I. G. Kevrekidis, H. H. Rotermund, and G. Ertl, "Pattern formation in composite excitable media," *Phys. Rev. E,* vol. 52, no. 6, pp. 5739–5742, 1995.
[11] K. J. Lee, E. C. Cox, and R. E. Goldstein, "Competing patterns of signaling activity in dictiostelium discoideum," *Phys. Rev. Lett.,* vol. 76, pp. 1174–1177, 1996.
[12] J. P. Keener, "Propagation and its failure in coupled systems of discrete excitable cells," *SIAM J. Appl. Math.,* vol. 47, no. 3, pp. 556–573, 1987.
[13] V. Pérez-Munuzuri, V. Pérez-Villar, and L. O. Chua, "Propagation failure in linear arrays of Chuas circuits," *Int. J. Bifurcation Chaos,* vol. 2, pp. 403–406, 1992.
[14] *Discretely-Coupled Dynamical Systems,* V. Pérez-Villar, V. Pérez-Munuzuri, L. O. Chua, and M. Markus, Eds. New York: World Scientific, 1996.
[15] A. P. Munuzuri, V. Pérez-Munuzuri, and V. Pérez-Villar, "Spiral waves on a 2-D array of nonlinear circuits," *IEEE Trans. Circuits Syst.,* vol. 40, pp. 872–877, Nov. 1993.
[16] A. P. Munuzuri, V. Pérez-Munuzuri, M. Gómez-Gesteira, L. O. Chua, and V. Pérez-Villar, "Spatiotemporal structures in discretely-coupled arrays of nonlinear circuits: a review," *Int. J. Bifurcation Chaos,* vol. 5, pp. 17–50, 1995.
[17] V. Pérez-Munuzuri, A. P. Munuzuri, M. Gómez-Gesteira, V. Pérez-Villar, L. Pivka, and L. O. Chua, "Nonlinear waves, patterns and spatio-temporal chaos in cellular neural networks," *Philos. Trans. R. Soc. London A, Math. Phys. Sci.,* vol. 353, pp. 101–113, 1995.
[18] A. P. Munuzuri, M. deCastro, E. Hofer, V. Pérez-Munuzuri, M. Gómez-Gesteira, and V. Pérez-Villar, "Continuous conductive volume affects the propagation of signals in dicrete systems," *Int. J. Bifurcation Chaos,* vol. 6, no. 10, pp. 1829–1835, 1996.
[19] V. Pérez-Munuzuri, M. Alonso, and V. Pérez-Villar, "Resonance patterns in one-dimensional arrays of coupled nonlinear excitable systems," *Int. J. Bifurcation Chaos,* vol. 4, no. 6, pp. 1631–1638, 1994.
[20] I. P. Marino, M. deCastro, V. Pérez-Munuzuri, M. Gómez-Gesteira, L. O. Chua, and V. Pérez-Villar, "Study of reentry initiation in coupled parallel fibers," *IEEE Trans. Circuits. Syst.,* vol. 42, pp. 665–671, Oct. 1995.
[21] M. deCastro, M. Gómez-Gesteira, and V. Pérez-Villar, "Influence of the distance on the interaction between an autonomous pacemaker and a reentry," *Phys. Rev. E.,* vol. 57, no. 1, pp. 949–954, 1998.
[22] R. N. Madan, *Chuas Circuit: A Paradigm for Chaos* (Series on Nonlinear Science) New York: World Scientific, 1993, vol. 1.
[23] L. O. Chua "The genesis of Chuas circuit," *Int. J. Elec. and Commun.,* vol. 46, pp. 250–257, 1992.
[24] A. S. Mikhailov, *Foundations of Synergetics I.* Berlin, Germany: Springer–Verlag, 1990.
[25] J. J. Tyson and J. P. Keener, "Singular perturbation theory of traveling waves in excitable media (a review)," *Physica D,* vol. 32, pp. 327–361, 1988.
[26] J. Brugada, L. Boersma, Ch. Kirchhof, and M. Allessie, "Double wave reentry as a mechanism of ventricular tachycardia acceleration during programmed electrical stimulation," *Circulation,* vol. 81, pp. 1633–1643, 1990.
[27] M. A. Allessie, M. J. Schalij, Ch. Kirchhof, *et al.,* "Experimental electrophysiology and arrhythmogenecity. Anisotropy and ventricular tachycardia," *Eur. Heart J.,* vol. 10, pp. 8–14, 1989.
[28] V. S. Zykov, *Simulation of Wave Processes in Excitable Media.* Manchester, U.K.: Manchester Univ. Press, 1987.
[29] V. A. Davydov and V. S. Zykov,"Spiral autowaves in a round excitable medium," *JETP,* vol. 76, no. 3, pp. 414–419, 1993.